Article

A Complete Set of NMR Chemical Shifts and Spin–Spin Coupling Constants for l-Alanyl-l-alanine Zwitterion and Analysis of Its Conformational Behavior

Petr Bou, Milo Budnsk, Vladimr pirko, Josef Kapitn, Jaroslav ebestk, and Vladimr Sychrovsk

J. Am. Chem. Soc., **2005**, 127 (48), 17079-17089• DOI: 10.1021/ja0552343 • Publication Date (Web): 11 November 2005

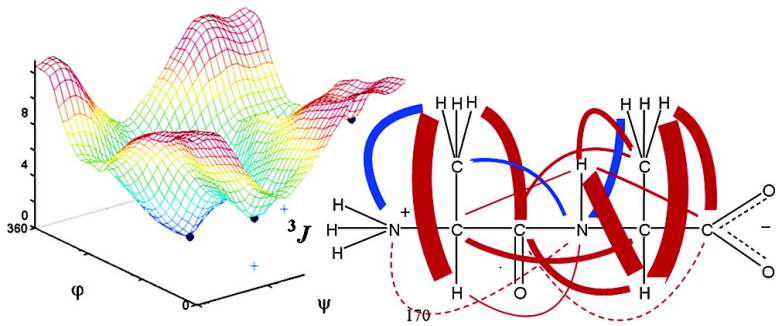

More About This Article

Additional resources and features associated with this article are available within the HTML version:

- Supporting Information
- Links to the 7 articles that cite this article, as of the time of this article download
- Access to high resolution figures
- Links to articles and content related to this article
- Copyright permission to reproduce figures and/or text from this article

View the Full Text HTML

J|A|C|S
ARTICLES
Published on Web 11/11/2005

A Complete Set of NMR Chemical Shifts and Spin−Spin Coupling Constants for L-Alanyl-L-alanine Zwitterion and Analysis of Its Conformational Behavior

Petr Bouř,* Miloš Buděšínský,* Vladimír Špirko,* Josef Kapitán, Jaroslav Šebestík, and Vladimír Sychrovský*

Contribution from the Institute of Organic Chemistry and Biochemistry, Academy of Sciences of the Czech Republic, Flemingovo nám. 2, 16610, Praha 6, Czech Republic

Received August 16, 2005; E-mail: bour@uochb.cas.cz; budesinsky@uochb.cas.cz; spirko@uochb.cas.cz; sychrovsky@uochb.cas.cz

Abstract: With the aid of labeling with stable isotopes (^{15}N and ^{13}C) a complete set of chemical shifts and indirect spin−spin coupling constants was obtained for the zwitterionic form of L-alanyl-L-alanine in aqueous solution. Different sensitivities of the NMR parameters to the molecular geometry were discussed on the basis of comparison with ab initio (DFT) calculated values. An adiabatic two-dimensional vibrational wave function was constructed and used for determination of the main chain torsion angle dispersions and conformational averaging of the NMR shifts and coupling constants. The quantum description of the conformational dynamics based on the density functional theory and a polarizable continuum solvent model agrees reasonably with classical molecular dynamics simulations using explicit solvent. The results consistently evidence the presence of a single form in the aqueous solution with equilibrium main chain torsion angle values ($\psi = 147°$, $\varphi = -153°$), close to that one found previously in an X-ray study. Under normal temperature the torsion angles can vary by about 10° around their equilibrium values, which leads, however, to minor corrections of the NMR parameters only. The main chain heavy atom chemical shifts and spin−spin coupling constants involving the α-carbon and hydrogen atoms appear to be most useful for the peptide structural predictions.

Introduction

Small molecules which model fundamental parts and properties of peptides and proteins become increasingly popular because they can be well manipulated and their accurate theoretical analysis is still feasible. For example, unique knowledge of structure, flexibility, and solute−solvent interactions was obtained recently for *N*-methylacetamide,[1,2] alanine,[3,4] diglycin,[5,6] alanine diamide,[7] and other peptide building blocks.[8−13] The L-alanyl-L-alanine (LALA) molecule itself, one of the simplest chiral peptides, appears particularly challenging because of its strong interaction with the solvent. As a matter of fact, the neutral zwitterionic form cannot exist in a vacuum, as was confirmed by theoretical[14] and experimental[15] studies. Similar attention was devoted also to other charged forms of L-alanyl-L-alanine.[16] Despite numerous investigations of LALA,[14,15,17−20] no definite conclusion concerning LALA conformation and dynamics in solution was deduced because of the limited accuracy of the simulation techniques. Although previous studies suggested rather semirigid conformation,[14,18] the usual approach may not have been adequate for description of the torsional motions opposed by soft potentials. Knowledge of such torsional flexibility can enlighten peptide biological activity[21] and has additional implications important for a correct determination of the peptide structures from the NMR data. Thus we find it worthwhile to analyze the conformational dependence of the chemical shifts and spin−spin coupling constants of LALA in the framework of a two-dimensional (2D) torsional model. Using

(1) Torii, H. *J. Phys. Chem. A* **2004**, *108*, 7272−7280.
(2) Ham, S.; Kim, J. H.; Kochan, L.; Cho, M. *J. Chem. Phys.* **2003**, *118*, 3491−3498.
(3) Park, S. W.; Ahn, D. S.; Lee, S. *Chem. Phys. Lett.* **2003**, *371*, 74−79.
(4) Selvarengan, P.; Kolandaivel, P. *THEOCHEM* **2004**, *671*, 77−86.
(5) Nandini, G.; Sathyanarayana, D. N. *J. Phys. Chem. A* **2003**, *117*, 11391−1140.
(6) Xu, S.; Nilles, J. M.; Bowen, K. H. J. *J. Chem. Phys.* **2003**, *119*, 10696−10701.
(7) Hudaky, I.; Hudaky, P.; Percel, A. *J. Comput. Chem.* **2004**, *25* (12), 1522−1531.
(8) Jalkanen, K. J.; Elstner, M.; Suhai, S. *THEOCHEM* **2004**, *675* (1−3), 61−77.
(9) Oboodi, M. R.; Alva, C.; Diem, M. *J. Phys. Chem.* **1984**, *88* (3), 501−505.
(10) Diem, M.; Oboodi, M. R.; Alva, C. *Biopolymers* **1984**, *23*, 1917−1930.
(11) Lee, O.; Roberts, G. M.; Diem, M. *Biopolymers* **1989**, *28*, 1759−1770.
(12) Mehta, M. A.; Fry, E. A.; Eddy, M. T.; Dedeo, M. T.; Anagnost, A. E.; Long, J. R. *J. Phys. Chem. B* **2004**, *108*, 2777−2780.
(13) Jacob, R.; Fischer, G. *J. Phys. Chem. A* **2003**, *107*, 6136−6143.
(14) Bouř, P.; Kapitán, J.; Baumruk, V. *J. Phys. Chem. A* **2001**, *105*, 6362−6368.
(15) Knapp-Mohammady, M.; Jalkanen, K. J.; Nardi, F.; Wade, R. C.; Suhai, S. *Chem. Phys.* **1999**, *240*, 63−77.
(16) Lucas, B.; Gregoire, H.; Maitre, P.; Ortega, J. M.; Rupenyan, A.; Reimann, B.; Scherman, J. P.; Desfrancois, C. *Phys. Chem. Chem. Phys.* **2004**, *6*, 2659−2663.
(17) Diem, M.; Lee, O.; Roberts, G. M. *J. Phys. Chem.* **1992**, *96*, 548−554.
(18) Jalkanen, K. J.; Nieminen, R. M.; Knapp-Mohammady, M.; Suhai, S. *Int. J. Quantum Chem.* **2003**, *92* (2), 239−259.
(19) Weir, A. F.; Lowrey, A. H.; Williams, R. W. *Biopolymers* **2001**, *58*, 577−591.
(20) Zuk, W. M.; Freedman, T. B.; Nafie, L. A. *Biopolymers* **1989**, *28*, 2025−2044.
(21) Peterson, J. R.; Bickford, L. C.; Morgan, D.; Kim, A. S.; Ouerfelli, O.; Kirschner, M. W.; Rosen, M. K. *Nat. Struct. Mol. Biol.* **2004**, *11*, 747−755.

the 2D property surfaces for the shifts and indirect coupling constants, the torsion angle φ, ψ values can be determined by comparing with experimental values.

Though the NMR spectroscopy is routinely used to probe molecular structure,[22−28] interpretation of the spectra based on the first principles became feasible only lately by efficient implementations of the coupled-perturbed techniques generally available software. Especially the density functional theory (DFT) methods thus have significantly reduced computer cost for the calculation of the chemical shifts and indirect NMR spin−spin coupling constants for systems of biochemical interest.[29−34] Reliable calculation of the NMR parameters is feasible for systems such as nucleic acid bases,[35,36] porphyrins,[37] or fullerenes.[38] Traditionally, the relation between the spin−spin coupling constants and molecular structures is described by empirical Karplus-type relations.[39−44] It is, however, problematic to apply these equations for compounds chemically different from those ones used for their calibration.[45,46] In such a situation it is more suitable to use ab initio analysis which provides more reliable estimates of the sensitivity of various types of the constants on the molecular conformation.

The resolution of molecular structure on the basis of comparison of calculated NMR parameters with experiment is not straightforward and may be affected by a number of factors including accuracy of the calculation,[29] the effect of solvent and averaging of molecular motion (as shown, for example, in refs 37 and 46−48). In the case of longer peptides and proteins the number of the spin−spin coupling constants becomes very large and not all of them can be used for reliable structural analysis. Thus constants suitable for the measurement can be selected conveniently by means of the ab initio calculations.

In LALA, as in most peptides, conformational dynamics is governed mostly by the main chain torsions which can be assumed to be adiabatically separable from the remaining molecular movements. In other words changes of the LALA molecular shape can be described using a two-dimensional torsional Schrödinger equation and the sought structural characteristics can be obtained by averaging over corresponding wave functions. Note also that the previous molecular dynamics (MD) studies indicate that the usual vibrational averaging based on the harmonic approximation is problematic for simple peptides exhibiting large-amplitude vibrations.[49] An alternative approach can be based, for example, on conventional or quantum molecular-dynamics simulations. To complete our study, the theoretical chemical shift and spin−spin coupling constants are thus compared to experimental data, and the conformational dependence of the NMR parameters on the main chain angles is analyzed and possible generalization for peptide structural analyses is suggested. We suppose that internal rotational motions of the CH_3, NH_3^+, and CO_2^- groups do not change the peptide secondary structure and that NMR parameters of rotating atoms can be replaced by an average value due to their fast movements.[50]

Experiment

Synthesis of Isotopically Labeled Dipeptide. A series of isotopically labeled dipeptides H-Ala-Ala-OH was prepared from isotopically labeled alanine compounds (L-Alanine (^{15}N, 98%) and L-Alanine (^{13}C, 98%; ^{15}N, 98%) purchased from Stable Isotopes, Inc. Conventional peptide synthesis in solution was employed with maximization of the reaction efficiencies. In the first step, the benzyloxycarbonyl (Z) protection group was introducted by treatment with *N*-benzyloxycarbonyloxysuccinimide.[51] Then the protected alanine was converted to its active ester with DCC and *N*-hydroxysuccinimide.[52] After aminolysis of the prepared active ester with unprotected labeled alanine, the zwitterionic dipeptide was obtained by hydrogenolysis on Pd-black[53] and purified by HPLC.

NMR Experiments. The NMR spectra of nonlabeled L-Ala-L-Ala, ^{15}N labeled l-Ala(^{15}N)-L-Ala(^{15}N), and fully ^{15}N- and ^{13}C-labeled L-Ala-(^{13}C,^{15}N)-L-Ala(^{13}C,^{15}N) were measured with FT NMR spectrometers Varian UNITY-500 and Bruker AVANCE-500 (^{1}H at 500 MHz, ^{13}C at 125.7 MHz, ^{15}N at 50.7 MHz, ^{17}O at 67.8 MHz) in D_2O and/or in the mixture H_2O/D_2O (9:1). All spectra were measured at room temperature except for the ^{17}O NMR spectrum which was recorded at 80°C. Chemical shifts were referenced to either internal (DSS for ^{1}H and ^{13}C; H_2O for ^{17}O) or external (nitromethane in the capillary for ^{15}N) standards. The nonlabeled compound was used to determine ^{1}H, ^{13}C, and ^{17}O chemical shifts and J(H,H) and J(C,H) couplings. The structural assignment of the hydrogen and carbon chemical shifts was achieved using homonuclear two-dimensional 2D-^{1}H pulse field gradient correlation spectroscopy (^{1}H-PFG-COSY) and heteronuclear 2D-^{1}H pulse field gradient heteronuclear single-quantum coherence (^{13}C-PFG-HSQC) and 2D-^{1}H pulse field gradient heteronuclear multibond correlation (^{13}C-PFG-HMBC) experiments in D_2O. The solvent mixture

(22) Roberts, G. C. K. *NMR of Macromolecules*; IRL: Oxford, 1993.
(23) Wüthrich, K. *NMR of Proteins and Nucleic Acids*; Wiley: New York, 1986.
(24) Evans, J. N. S. *Biomolecular NMR Spectroscopy*; Oxford University Press: Oxford, 1995.
(25) Dobson, C. M. NMR and Protein Folding: Studies of Lysozyme and alpha-Lactalbumin. *Protein Conformation (CIBA Foundation Symposium 161)*; Wiley: Chichester, 1991; p 167.
(26) Cavanagh, J.; Fairbrother, W. J.; Palmer, A. G., III; Skelton, N. J. *Protein NMR Spectroscopy*; Academic Press Inc.: San Diego, 1995.
(27) Smith, L. J.; Dobson, C. M. *Int. J. Quantum Chem.* **1996**, *59*, 315−332.
(28) Eberstadt, M.; Gemmecker, G.; Mierke, D. F.; Kessler, H. *Angew. Chem., Int. Ed. Engl.* **1996**, *34* (16), 1671−1695.
(29) Helgaker, T.; Jaszunski, M.; Ruud, K. *Chem. Rev.* **1999**, *99* (1), 293−352.
(30) Malkina, O. L.; Malkin, V. G. *Angew. Chem., Int. Ed.* **2003**, *42* (36), 4335−4338.
(31) Sychrovský, V.; Gräfenstein, J.; Cremer, D. *J. Chem. Phys.* **2000**, *113*, 3530−3547.
(32) Helgaker, T.; Watson, M.; Handy, N. C. *J. Chem. Phys.* **2000**, *113* (21), 9402−9409.
(33) Schreckenbach, G.; Ziegler, T. *J. Phys. Chem.* **1995**, *99* (2), 606−611.
(34) Tomena, C. F.; Rittner, R.; Contreras, R. H.; Peralta, J. E. *J. Phys. Chem. A* **2004**, *108* (38), 7762−7768.
(35) Barfield, M.; Dingley, A. J.; Feigon, J.; Grzesiek, S. *J. Am. Chem. Soc.* **2001**, *123* (17), 4014−4022.
(36) Šponer, J. E.; Sychrovský, V.; Hobza, P.; Šponer, J. *Phys Chem. Chem. Phys.* **2004**, *6* (10), 2772−2780.
(37) Bernátková, M.; Dvořáková, H.; Andrioletti, B.; Král, V.; Bouř, P. *J. Phys. Chem. A* **2005**, *109*, 5518−5526.
(38) Jaszunski, M.; Ruud, K.; Helgaker, T. *Mol. Phys.* **2003**, *101* (13), 1997−2002.
(39) Haasnoot, C. A. G.; de Leeuw, F. A. A. M.; de Leeuw, H. P. M.; Altona, C. *Org. Magn. Reson.* **1981**, *15*, 43−52.
(40) Miranker, A.; Radford, S. E.; Karplus, M.; Dobson, C. M. *Nature* **1991**, *349*, 633−636.
(41) Brooks, C. L., III; Karplus, M.; Pettitt, B. M. *Proteins: a theoretical perspective of dynamics, structure and thermodynamics*. John Wiley & Sons: New York, 1988; Vol. LXXI.
(42) Smith, L. J.; Bolin, K. A.; Schwalbe, H.; Macarthur, M. W.; Thornton, J. M.; Dobson, C. M. *J. Mol. Biol.* **1996**, *255*, 494−506.
(43) Ratajczyk, T.; Pecul, M.; Sadlej, J.; Helgaker, T. *J. Phys. Chem. A* **2004**, *108*, 2758−2769.
(44) Wu, A. N.; Cremer, D.; Auer, A. A.; Gauss, J. *J. Phys. Chem. A* **2002**, *106*, 657−667.
(45) Hu, J. S.; Bax, A. *J. Am. Chem. Soc.* **1997**, *119*, 6360−6368.
(46) Bouř, P.; Raich, I.; Kaminský, J.; Hrabal, R.; Čejka, J.; Sychrovský, V. *J. Phys. Chem. A* **2004**, *108*, 6365−6372.
(47) Sebastiani, D.; Rothlisberger, U. *J. Phys. Chem. B* **2004**, *108*, 2807−2815.
(48) Bouř, P.; Sychrovský, V.; Maloň, P.; Hanzlíková, J.; Baumruk, V.; Pospíšek, J.; Buděšínský, M. *J. Phys. Chem. A* **2002**, *106*, 7321−7327.
(49) Kamiya, N.; Watanabe, Y. S.; Ono, S.; Higo, J. *Chem. Phys. Lett.* **2005**, *401*, 312−317.
(50) Sandstrom, J. *Dynamic NMR Spectroscopy*; Academic Press: London, 1982.
(51) Cheng, L.; Goodwin, C. A.; Schully, M. F.; Kakkar, V. V. *J. Med. Chem.* **1992**, *35* (18), 3364−3369.
(52) Wünsch, E.; Wendlberger, G.; Deimer, K. H. *Hoppe-Seyler's Z. Physiol. Chem.* **1976**, *357* (3), 447−458.
(53) Stein, W. H.; Moore, S.; Bergmann, M. *J. Biol. Chem.* **1944**, *154*, 191−201.

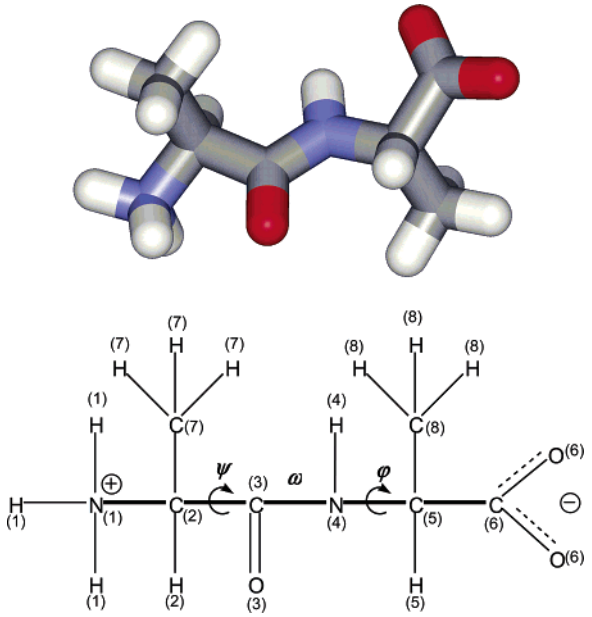

Figure 1. Calculated (BPW91/PCM/6-311++G**) lowest-energy geometry of LALA (conformer **A**) and the atom numbering used for the description of chemical shifts and the coupling constants. Hydrogen and oxygen numbers correspond to the connected heavy atoms.

H_2O/D_2O (9:1) was used to observe the signals of NH and NH_3^+ protons. Only the couplings of amide NH could be observed in this mixture because of the high exchange rate of amine NH_3^+ protons with water. The *J*(H,H) values were determined from 1D-^{1}H NMR spectrum and *J*(C,H) couplings from a nondecoupled 1D-^{13}C NMR spectrum. A series of selective ^{1}H-decoupled ^{13}C NMR spectra was used to assign individual *J*(C,H) couplings. The ^{17}O chemical shifts were obtained at 80 °C (to narrow very broad ^{17}O lines) and assigned tentatively to NHCO and COOH according to the signal intensities and known relative shift values of these groups. The labeled ^{15}N and ^{15}N,^{13}C L-Ala-L-Ala samples were used mainly for obtaining *J*(N,H), *J*(N,C), and *J*(C,C) coupling constants using 1D-^{1}H and ^{13}C NMR spectra, 1D-^{13}C-INADEQUATE (Incredible Natural Abundance Double Quantum Transfer Experiment) and 2D-^{1}H,^{15}N-PFG-HMBC spectra.

Calculations

Geometries. A two-dimensional potential energy surface (PES) of LALA was obtained by scanning the main chain torsion angles φ, ψ defined in Figure 1. The scan was performed at the BPW91[54,55]/6-311++G** level in conjunction with the PCM[56] and COSMO[57,58] continuum water models as implemented in the Gaussian program package.[59] The COSMO surface (as well as those obtained by control computations utilizing the Becke3LYP functional and/or a smaller basis, 6-31G**) was found quite similar to PCM and is not analyzed further. First, the angles φ, ψ were scanned with a step of 60°, and then other geometries in vicinities of the minima were added to the total of about 80 points. Finally, an analytical surface was obtained by a fitting with polynomials. The scans were started with the *trans*-conformation of the amide group ($\omega = 180°$) because no experimental data indicate the presence of the *cis*-conformer. But the angle ω was not constrained,

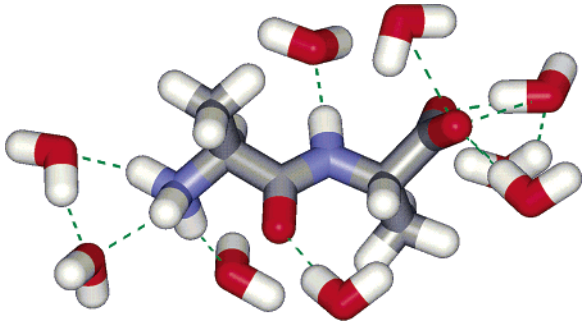

Figure 2. Geometry of the LALA zwitterion solvated with 9 water molecules of the first hydration sphere. Hydrogen bonds are marked by the dashed green lines.

and all coordinates except φ and ψ were fully optimized at each point. To check the influence of explicit hydrogen bonding not included in the PCM model, explicit water molecules were added to LALA in a vacuum (the geometry is displayed in Figure 2) and in combination with the PCM model for outer hydration shells. Probable positions of the solvent molecules were selected using the Tinker[60] molecular dynamics (MD) program package from an MD simulation of LALA in a water box.

NMR Parameters. Chemical shifts and the indirect spin−spin coupling constants were calculated analytically by Gaussian using the GIAO method[61−63] with the Becke3LYP[64] functional, as this approach was found suitable for analogous computations previously.[31,32] All four important contributions, diamagnetic spin−orbit, paramagnetic spin−orbit, Fermi contact, and spin dipolar, were included, and an extended set of atomic orbitals was used: the (9s,5p,1d/5s,1p) [6s,4p,1d/3s,1p] bases for carbon and nitrogen, the (5s,1p) [3s,1p] basis for hydrogen (referred to as IGLO II), and in some cases also a larger set (11s,7p,2d/6s,2p) [7s,6p,2d/4s,2p] (IGLO III), all of them proposed for computation of magnetic properties previously.[65] The same PCM solvent correction was used as in the case of the geometry surfaces. The property surfaces, dependencies of the chemical shifts and coupling constants on the conformation, were obtained analogously as was the energy by a scan over the angles φ and ψ.

Molecular Dynamics. Alternatively to the ab initio PES mapping, we performed a molecular dynamic (MD) simulation of the LALA molecule in a box containing 502 water molecules using the AMBER program package.[66] The Amber94,[67] Amber99,[68] and Amber03[69] peptide force fields of AMBER and the Charmm27[70] field of Tinker[60,71] were applied with the periodic boundary conditions, constant pressure of 1 atm, a temperature of 300 K, a weak-coupling algorithm,[72] a nonbonded cutoff of 8 Å, and the TIP3P water model.[73] A time step of 1 fs was used for integration of the Newton equations, and the trajectory

(54) Becke, A. D. Exchange-correlation approximations in density-functional theory. In *Modern electronic structure theory*; Yarkony, D. R., Ed. World Scientific: Singapore, 1995; Vol. 2, pp 1022−1046.
(55) Becke, A. *Phys. Rev. A* **1988**, *38*, 3098−3100.
(56) Cammi, R.; Mennucci, B.; Tomasi, J. *J. Phys. Chem. A* **2000**, *104*, 5631−5637.
(57) Klamt, A. *J. Phys. Chem.* **1995**, *99*, 2224−2235.
(58) Klamt, A. COSMO and COSMO-RS. In *The Encyclopedia of Computatinal Chemistry*; Schleyer, P. R., Allinger, N. L., Clark, T., Gasteiger, J., Kollman, P. A., Schaefer, H. F., III, Schreiner, P. R., Eds. John Wiley & Sons: Chichester, 1998; Vol. 1, pp 604−615.
(59) Frisch, M. J. at al. *Gaussian 03*; Gaussian, Inc.: Pittsburgh, PA, 2003.
(60) Ponder, J. W. *Tinker*, version 3.8; Washington University School of Medecine: Saint Louis, MS, 2000.
(61) Ditchfield, R. *Mol. Phys.* **1974**, *27*, 789−807.
(62) Dodds, J. L.; McWeeny, R.; Sadlej, A. J. *Mol. Phys.* **1980**, *41*, 1419−1430.
(63) Wolinski, K.; Hilton, J. F.; Pulay, P. *J. Am. Chem. Soc.* **1990**, *112*, 8251−8260.
(64) Becke, A. D. *J. Chem. Phys.* **1993**, *98*, 5648−5652.
(65) Kutzelnigg, W.; Fleischer, U.; Schindler, M. *NMR − Basis Principles and Progress*; Springer: Heidelberg, 1990.
(66) Pearlman, D. A.; Case, D. A.; Caldwell, J. W.; Ross, W. S.; Cheatham, T. E.; Debolt, S.; Ferguson, D. M.; Seibel, G.; Kollman, P. A. *Comput. Phys. Commun.* **1995**, *91*, 1−41.
(67) Cornell, W. D.; Cieplak, P.; Bayly, C. I.; Gould, I. R.; Merz, K. M.; Ferguson, D. M.; Spellmeyer, D. C.; Fox, T.; Caldwell, J. W.; Kollman, P. A. *J. Am. Chem. Soc.* **1995**, *117*, 5179−5197.
(68) Wang, J.; Cieplak, P.; Kollman, P. A. *J. Comput. Chem.* **2000**, *21*, 1049−1074.
(69) Duan, Y.; Wu, C.; Chowdhury, S.; Lee, M. C.; Xiong, G.; Zhang, W.; Yang, R.; Cieplak, P.; Luo, R.; Lee, T. *J. Comput. Chem.* **2003**, *24*, 1999−2012.
(70) Foloppe, N.; MacKerell, A. D. *J. Comput. Chem.* **2000**, *21*, 86−104.
(71) Ren, P.; Ponder, W. *J. Phys. Chem. B* **2003**, *107*, 5933−5947.
(72) Berendsen, H. J. C.; Postma, J. P. M.; van Gunsteren, W. F.; Dinola, A.; Haak, J. R. *J. Chem. Phys.* **1984**, *81*, 3684−3690.

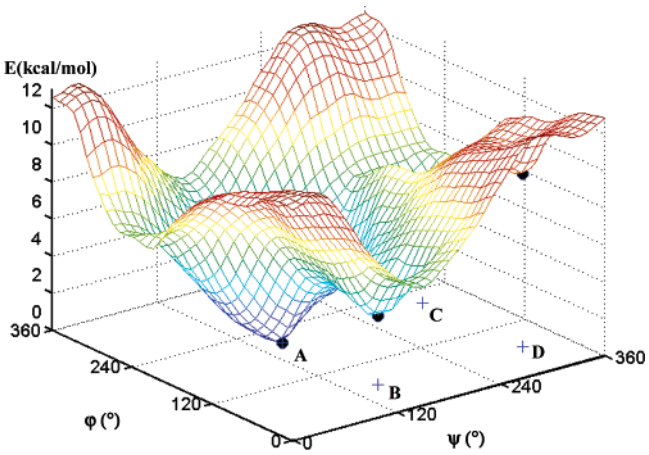

Figure 3. Dependence of relative conformer energy of the LALA zwitterion in water on the main chain torsion angles as calculated at the Becke3LYP/6-311++G**/PCM level. The minima **A**−**D**, dots (●) on the surface and crosses (+) at the φ,ψ plane projection, correspond to those in Table 1.

coordinates and free-energies were recorded every 1 ps within a total simulation time of 20 ns and analyzed by a software written by us.

Vibrational Dynamics. The quantum and quantum dynamical effects of the torsional motions involving the angles (φ, ψ) were studied using an approximate Hamiltonian,

$$H = \frac{1}{2}\sum_{\alpha,\beta} G_{\alpha\beta}(\varphi,\psi)P_\alpha P_\beta + V(\varphi,\psi) \qquad (1)$$

where $P_\gamma = -i\hbar\partial/\partial\gamma$ ($\gamma = \varphi,\psi$), $V(\varphi,\psi)$ is the potential energy function, and $G_{\alpha\beta}$ are matrix elements of the generalized vibrational kinematic matrix.[74] The eigenvalue problem $H\Psi = E\Psi$ was solved variationally in basis set functions expressed as products of the eigenfunctions of the corresponding uncoupled one-dimensional Schrödinger equations. The one-dimensional functions were determined numerically using the Numerov−Cooley integration procedure.[75] Average values of the NMR parameters for each state i were calculated as the expectation values

$$\langle g_i \rangle = \langle \Psi_i(\varphi,\psi)|g(\varphi,\psi)|\Psi_i(\varphi,\psi)\rangle \qquad (2)$$

where $g(\varphi,\psi)$ are theoretically evaluated surfaces of the studied properties (shifts, couplings). For selected localized excited vibrational states their lifetimes were estimated from simplified one-dimensional modeling described below.

Results and Discussion

Potential Energy Surface. Despite the strong interaction with the solvent and the presence of the rotating single covalent bonds, only one conformation (**A**) viable under normal conditions was found by the BPW91/6-311++G**/PCM method. The other three local minima (**B**−**D**) on the adiabatic two-dimensional potential energy surface (Figure 3, Table 1) cannot be significantly populated at room temperature. The equilibrium torsion angles $(\varphi,\psi) = (-153°, 147°)$ pertaining to the studied conformers are collected in Table 1. The prevalence of conformer **A** is in agreement with the X-ray data (Table 1)[76] and also with previous Raman optical activity[14] and other ab initio studies.[15] Note, that explicit hydrogen bonding not included in our PCM model may lead to a certain stabilization of different forms of the molecule.[18] We thus realize that our results can be affected by this simplification.

Table 1. Geometries and Relative Conformer Energies of LALA Obtained by Various Techniques

conformer		φ (deg)	ψ (deg)	E (kcal/mol)
	This Work			
BPW91/ 6-311++G**/PCM				
A		−153	147	0.0
B		67	150	3.7
C		−150	−50	5.2
D		64	−45	9.3
MD simulation				
(A)	Amber99[68]	−150	145	
(A)	Amber94[67], Amber03[69]	−65	145	
(A)	Charmm27[70]	−90	175	
	Other Works			
A	X-ray[76]	−113	165	
A	B3LYP/6-31G*/Onsager[15]	−170	172	
A	BPW91/6-311G**/COSMO[14]	−162	179	
E	B3LYP/6-31G*/Onsager, cluster with 14 H_2Os[18]	−65	−164	

Interestingly, similar MD equilibrium structures as those for LALA were obtained also for a similar but neutral diamide (Ac-Ala-NMe).[77,78] Thus, we can speculate that the influence of the charged ends on the zwitterion conformation is significantly reduced by water. Various MD force fields, however, provide different average conformations (cf. Table 1) only vaguely related to the conformer **A** obtained ab initio. The Amber family force fields (Amber94, Amber99 and Amber03) lead to two variously populated conformers with the same ψ (∼ 145°) but different φ (−150° and −65°) angles, while only one minimum on the free energy surface was obtained by the Charmm27 force field with average angles ($\psi = 175°$, $\varphi = -90°$). Supposedly, these results are inferior to the Becke3LYP/6-311++G**/PCM ab initio prediction, because the MD force field was developed rather for longer peptides and proteins.

It is nevertheless remarkable that the probability conformer distribution obtained from molecular dynamics reasonably agrees with the quantum picture, as can be seen in Figure 4 where the probabilities obtained by the two approaches are compared. Although explicit hydrogen bonds and coupling with water motion somewhat stabilize rare conformers, the MD free-energy landscape (for the Amber99 force field) clearly leads to one prevalent conformation close to the conformer **A** obtained by ab initio computation. It should be stressed that the comparison is only qualitative because we are using only a simplified two-dimensional quantum model. Nevertheless, the torsion angle dispersions estimated for the lowest-vibrational states appear to be representative, at least as a lower limit of the dispersion. Apparently, the lowest-energy conformer (**A**) is well-stabilized by the potential well; however its flexibility is rather profound as the (φ, ψ) angles can almost freely vary within about ±10°. This behavior must be clearly taken into account when physical properties of the molecule are considered. In other words, the term "conformation" cannot be related to a classically rigid structure for LALA. We suppose that longer

(73) Jorgensen, W. L.; Chandrasekhar, J.; Madura, J. D. *J. Chem. Phys.* **1983**, *79*, 926−935.
(74) Čejchan, A.; Špirko, V. *J. Mol. Spectrosc.* **2003**, *217* (1), 142−145.
(75) Ixaru, L. *Numerical Methods for Differential Equations and Applications*; Reidel: Dordrecht, 1984.
(76) Fletterick, R. J.; Tsai, C.; Hughes, R. E. *J. Phys. Chem.* **1971**, *75* (7), 918−922.
(77) Gnanakaran, S.; Garcia, A. E. *J. Phys. Chem. B* **2003**, *107*, 12555−12557.
(78) Hu, H.; Elstner, M.; Hermans, J. *Proteins: Struct., Funct., Genet.* **2003**, *50*, 451−463.

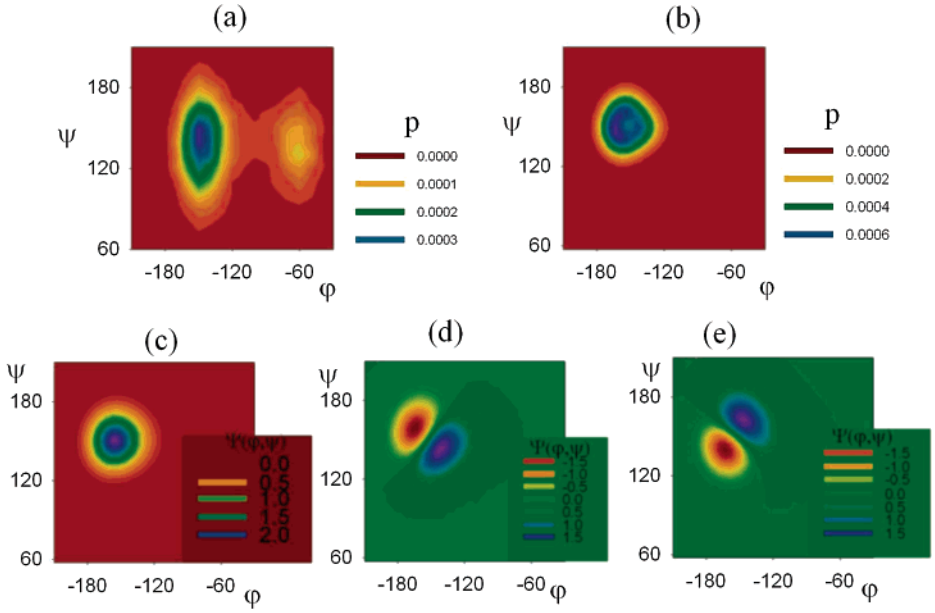

Figure 4. Probability conformer distribution as a function of the torsion angles (φ, ψ) obtained by molecular dynamics simulation (a) and as a sum of probabilities of the first three quantum states obtained for the ab inito surface (b). The wave functions of the quantum states are plotted below (c, d, e, amplitudes are normalized to angles in radians).

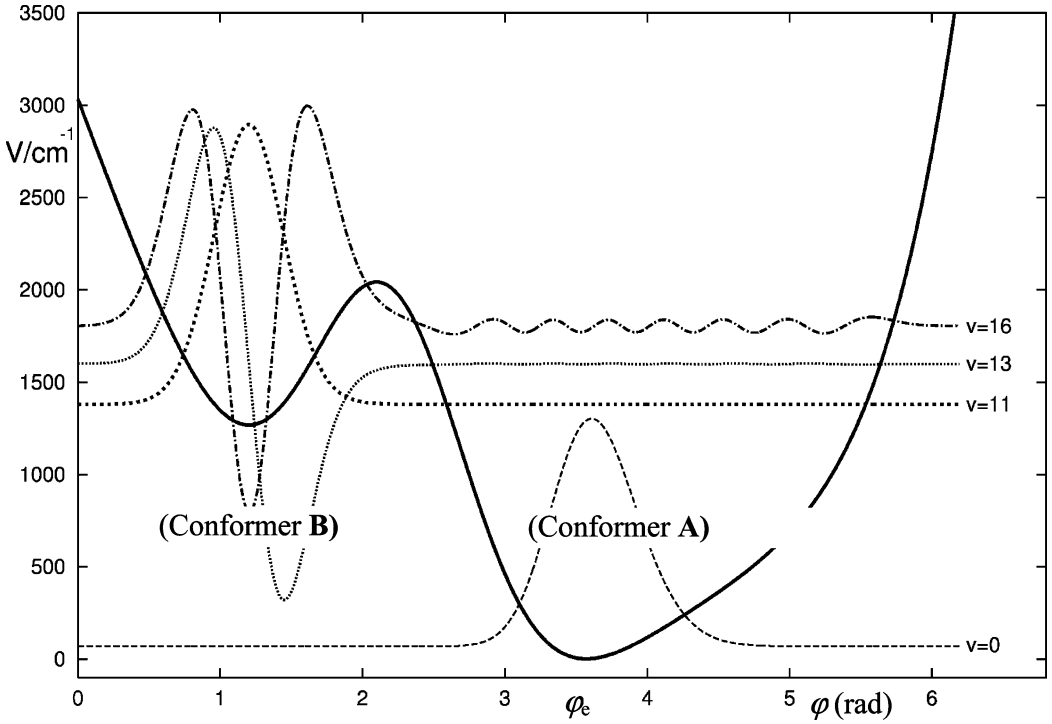

Figure 5. One-dimensional section of the potential energy surface from Figure 3 (solid line) and the eigenfunctions of the lowest ($v = 0$) and localized ($v = 11, 13, 16$) states of the φ-torsional motion.

peptides behave similarly, which can obviously contribute to the universality of their biological function. For LALA, the first two excited vibrational functions (d, e in Figure 4) which are nearly degenerate (with energies of 104 and 120 cm^{-1}) in the system reminds us of a two-dimensional harmonic oscillator[79] and suggests significant coupling of the rotations involving the two angles.

Lifetime of the Conformer B. From the four minima on the total potential energy function only two (**A**, **B**) are deep enough to support profoundly localized states. To estimate quantitatively the stability of the states trapped in the energetically higher potential energy well, we found it suitable to rely on the stabilization procedure ([80] and references therein). The actual calculations were performed by repeatedly diagonalizing the following one-dimensional Hamiltonians

$$H = \frac{1}{2}G_{\varphi}\varphi(\varphi)P_{\varphi}^{2} + V_i(\varphi)(i = 1,2) \qquad (3)$$

($V_1(\varphi) = V(\varphi)$; $V_2(\varphi) = V(\varphi)$ and 0 for $\varphi \leq \varphi_e$ and $\varphi > \varphi_e$,

(79) Papoušek, D.; Aliev, M. R. *Molecular Vibrational/Rotational Spectra*; Academia: Prague, 1982.

Table 2. Approximate Calculated Lifetimes of the Localized Vibrational States

	conformer A	conformer B		
	v = 0	v = 11	v = 13	v = 16
calc 1 ($V_1(\varphi)$)	∞	6 ms	10 μs	38 ps
calc 2 ($V_2(\varphi)$)	∞	11 ms	6 μs	40 ps

respectively) confined in a series of enclosing boxes $\varphi \in \langle 1.5,5.5rad \rangle$. The resulting energies form diagrams well stabilized for the values fairly close to the eigenvalues of the Hamiltonian involving unconfined potential $V(\varphi)$, and as a matter of fact, the wave functions of the confined states energetically coinciding with the stationary states of quantum numbers $v = 11,13$, and 16 are highly localized in the region of the higher minimum of $V(\varphi)$; see Figure 5. The stabilization diagrams provide practically the same lifetimes of these states (see Table 2) thus evidencing the fact that the decay of the states pertaining to the energetically richer conformer depends only on the potential energy barrier and can be thus described by means of the probed stabilization calculations.

Although the population of conformer **B** is presumably low under current experimental conditions, it may become important for other spectroscopic or scattering measurements. The lifetimes computed by the two stabilization calculations (Calc 1 and 2 in Table 2) reasonably coincide, and the lowest state ($v = 11$) even appears to live long enough (6−11 ms) to provide distinct NMR spectra. However, at present, we do not aim to carry out suitable experiments, and eventual detection of this conformer thus remains a challenge for future studies.

NMR Chemical Shifts. For the equilibrium structure (conformer **A**) the experimental and theoretical chemical shifts calculated at four ab initio levels are compared in Table 3. We estimate the absolute experimental errors as being about 0.01 ppm for hydrogen, 0.02 ppm for carbon, 1 ppm for nitrogen, and 4 ppm for the oxygen shifts. While the calculated shifts of carbon and hydrogen atoms reasonably agree with experiment, we observe larger deviations (∼25%) for the nitrogen and oxygen. This behavior has been described previously, especially the difficulties of the DFT theory to predict the nitrogen shift,[81] and cannot be easily improved. Better description of the influence of the polar environment and polarization of the free oxygen and nitrogen electron pair would require extensive computations including better electron correlation models and proper solvent treatment which is not feasible for a system of this size. Especially unpleasant is the switching of the relative magnitudes of the amide and carboxyl oxygen shifts when the explicit water molecules are included, which prevents trustable theoretical assignment. In this case, we suppose that the PCM model (second and third columns in the table) is more reliable since the water positions can be considered to be averaged, as the calculated difference in shifts of the two oxygens (16.6 ppm at the B3L/IGLOII/PCM level) agrees well with the observed value of 17.6 ppm. We suppose, however, that this does not contribute significantly to the overall error. More disturbing might be the elevated temperature that had to be used for the measurement of the oxygen chemical shift, influencing the internal rotation and overall dynamics of the CO_2^- group not included in our two-dimensional model. Similarly, the explicit and implicit solvent models are inconsistent in predicting the relative magnitudes of the carbons C2 and C5. In this case, however, relative shift changes are rather minor and, as shown later (Figure 7), also smaller than those caused by the conformation variations.

Table 3. Chemical Shifts (in ppm) Calculated for Conformer **A** at Four Levels of Approximation and the Experimental Values[a,b]

level:	B3L/IGLOII	B3L/IGLOIII	B3L/IGLOII	B3L/IGLOII	
solvent model:	PCM	PCM	explicit	PCM + explicit	expt
		Calculated Standard Shieldings:			
^{1}H (DSS)	31.83	31.53	31.83	31.83	
^{13}C (DSS)	183.45	181.10	183.45	183.45	
^{17}O (H_2O)	336.15	330.19	336.15	336.15	
^{15}N (CH_3NO_2)	−180.16	−194.36	−180.16	−180.16	
		LALA:			
H1	5.36	5.92	6.11	6.45	6.19
H2	4.37	4.86	3.22	3.88	4.07
H4	7.60	8.42	9.16	9.40	8.30
H5	4.02	4.69	4.17	4.01	4.15
H7	1.46	1.82	1.64	1.51	1.56
H8	1.17	1.62	1.30	1.25	1.36
C2	60.49	63.05	60.33	59.33	51.91
C3	175.39	181.28	174.15	179.57	172.81
C5	58.79	61.9	63.15	62.32	54.10
C6	185.32	192.46	186.11	190.16	182.53
C7	19.57	22.17	21.32	21.17	19.29
C8	22.79	24.28	27.02	26.27	19.95
N1	−378.8	−407.4	−393.7	−393.7	−334.10
N4	−276.5	−302.3	−286.5	−297.0	−254.65
O3	344.9	340.6	356.0	345.3	285.0
O6	328.3	324.8	379.3	361.4	267.4
Δ	24	29	36	33	0
Δ'	0.47	0.44	0.50	0.47	0

[a] Δ, Δ': the root-mean-square (RMS) errors (Δ' for hydrogens only). [b] Calculated standard shifts are obtained with BPW91/6-31G**/PCM equilibrium geometries (with water (for DSS, H_2O) and nitromethane (for nitromethane) as solvents), and the experimental shifts are referenced to internal (DSS for ^{1}H and ^{13}C; H_2O for ^{17}O) and external (nitromethane for ^{15}N) standards.

A much better agreement was achieved for the hydrogen and carbon chemical shifts, with an RMS error of ∼0.5 ppm for hydrogens (see Δ' in Table 3) and ∼5% for the carbons. The increase of the basis set size (IGLOII→IGLOIII) does not bring significant improvement of the results. Neither inclusion of the explicit water molecules improves agreement with experiment. Thus we can consider the B3L/IGLOII/PCM to be adequate and reliable enough for description of the carbon and hydrogen shifts and an unambiguous assignment of the experimental data. The somewhat larger variation of the amide group hydrogen (H4) shift reflects its known sensitivity on the solvent, concentration, and temperature. Possibly, an anharmonic behavior of the out of plane (pyramidal) nitrogen motion also somewhat influences the effective shift (Špirko et al., publication in preparation).

Spin−Spin Coupling Constants. All the constants involving one, two, and three bonds as schematically summarized in Figure 6 were determined for the natural dipeptide and with the aid of the isotopically labeled compounds. However, absolute magnitudes of several constants were below the instrument detection limit (∼1 Hz). As for absolute experimental error, we anticipate about a 0.1 Hz inaccuracy for the constants involving protons (J(H,H)), 0.3 Hz for J(C,H), and 0.5 Hz for the other couplings.

(80) Špirko, V.; Piecuch, P.; Bludský, O. *J. Chem. Phys.* **2000**, *112* (1), 189−202.
(81) Fadda, E.; Casida, M. E.; Salahub, D. R. *J. Phys. Chem. A* **2003**, *107*, 9924−9930.

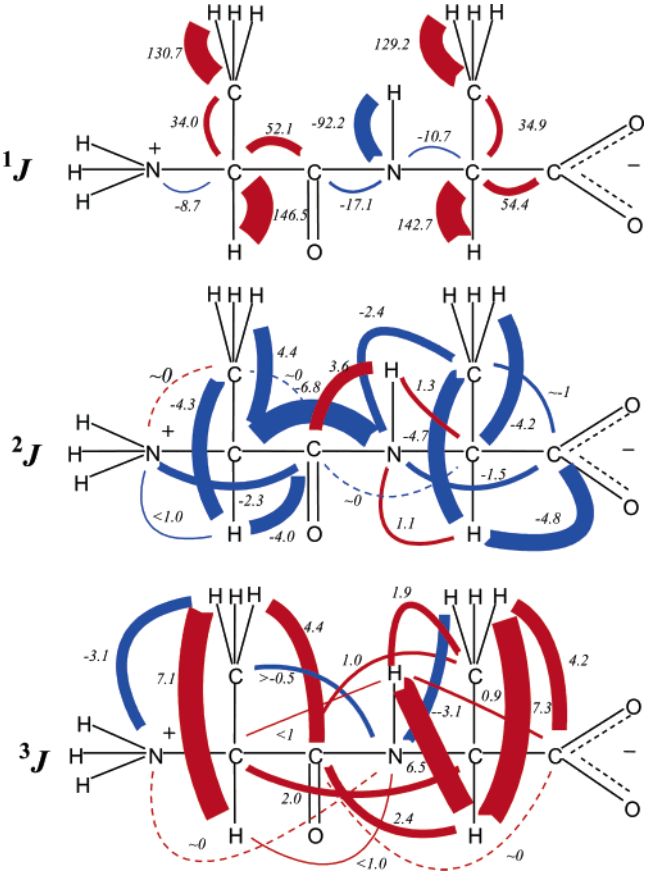

Figure 6. Overview of signs and relative magnitudes of the experimentally detectable spin−spin coupling constants in LALA.

It is noticeable that while the magnitudes of the one-bond constants are clearly the largest, the magnitudes become comparable for the two- and three-bond couplings (^1J, ^2J, ^3J). This probably reflects the nonlocality of the electric currents induced by the interacting nuclei.[82]

In detail the constants calculated with four model approximations are summarized and compared with the observed values in Table 4. In the sixth column of the table we also list a range of the constants previously observed in peptides.[83] We can see a good overall agreement between the theory and experiment (RMS errors < 2 Hz, relative errors smaller than 5−10%), usual for this level of approximation.[46] Nevertheless, similarly as for the shifts, a nonconvincing improvement is obtained by the basis set size increase and by the inclusion of the explicit water molecules (columns 3−5 in Table 4). The small differences in the constants obtained with and without the explicit solvent also indicate that the water position averaging may be less important than that for the shifts. Such lesser sensitivity of the coupling to the environment is in accord with previous experience.[36] Because most of the spin−spin coupling constants lie within the range observed for peptides (sixth column of the Table 4), we suppose that this observation can be generalized. However, the constants involving atoms in the vicinity of the polar molecular end (NH_3^+, CO_2^-) obviously deviate more from the standard peptide values.

With a lower accuracy than that for absolute values, but still correctly describing the trends, the differences in analogous

(82) Soncini, A.; P., L. *Chem. Phys. Lett.* **2005**, *409*, 177−186.
(83) Bystrov, V. F. *Prog. NMR Spectrosc.* **1976**, *10*, 41−81.

Table 4. Spin−Spin Coupling Constants (Hz) for the Conformer **A** Calculated at Four Levels, Peptide Literature and the Experimental Values

level: solvent model:	B3L/IGLOII PCM	B3L/IGLOIII PCM	B3L/IGLOII explicit	B3L/IGLOII PCM + explicit	peptides[b]	expt
			One-Bond Couplings (^1J)			
C7, H7	129.4	128.7	130.6	129.8	129	130.7
C8, H8	126.7	126.3	126.8	126.5	129	129.2
C2, H2	151.7	150.2	140.5	146.2	126	146.5
C5, H5	142.3	141.3	144.9	142.6	129	142.7
N4, H4	−92.1	−92.4	−90.8	−92.5	−89...−94.5	−92.2
C2, C3	53.0	50.7	54.4	55.5	50...53	52.1
C5, C6	53.6	51.9	56.0	57.7	50...53	54.4
C2, C7	35.0	33.1	34.3	34.6	32...38	34.0
C5, C8	36.7	34.6	35.9	36.4	32...38	34.9
C2, N1	−4.7	−4.4	−5.0	−5.4	−4.8...−11	−8.7
C3, N4	−19.6	−18.7	−17.8	−17.1	−12.9...−14.8	−17.1
C5, N4	−9.1	−8.7	−6.5	−8.3	−4.8...−11.0	−10.7
			Two-Bond Couplings (^2J)			
C2, H7	−3.2	−2.6	−3.1	−3.3		−4.4
C5, H8	−3.4	−2.8	−2.7	−2.9		−4.2
C5, H4	2.6	2.6	3.2	3.5	−2.5...−2.9	1.3
C3, H4	6.6	6.5	4.9	4.7	2.4...5.5	3.6
C7, H2	−2.8	−2.4	−2.4	−2.9	−4.6	−4.3
C8, H5	−3.4	−3.2	−1.3	−1.0	−4.6	−4.7
C3, H2	−3.1	−2.5	−3.8	−3.9	−4.2...−7.3	−4.0
C6, H5	−5.2	−4.7	−5.4	−5.3	−4.2...−7.3	−4.8
N1, H2	−0.7	0.6	0.9	−0.5	0...−2	<1[a]
N4, H5	0.3	0.1	0.5	0.8	0...−2	1.1[a]
C3, C5	−0.4	−0.3	−0.8	−0.5		∼0[a]
C3, C7	−0.9	−0.9	−1.2	−1.2	<1	∼0[a]
C6, C8	−0.7	−0.7	−0.6	−0.6	<1	∼1[a]
C7, N1	0.4	0.4	0.1	0.2	<1	∼1[a]
C2, N4	−10.5	−10.2	−10.0	−10.2	−6.6...-9.5	−6.8
C3, N1	−0.3	−0.3	−0.2	−0.1	−1.8	−2.3[a]
C8, N4	−0.4	−0.4	0.1	−0.2	<1	−2.4[a]
C6, N4	−0.5	−0.6	−0.6	−0.7	1.8	−1.5[a]
			Three-Bond Couplings (^3J)			
H4, H5	6.6	7.0	8.0	7.5	0.0.10.7	6.5
H2, H7	6.7	6.9	6.7	6.9	1.4...12.3	7.1
H5, H8	6.7	6.9	6.3	6.4	1.4...12.3	7.3
C2, H4	1.4	1.3	1.4	1.4	0...7.1	<1[a]
C6, H4	3.2	3.1	2.5	1.6	−0.2...6.0	0.9
C8, H4	0.0	0.0	0.0	0.2	1.9	1.9
C3, H7	4.2	4.1	4.2	4.5	1.9...6.7	4.4
C6, H8	3.9	3.9	3.9	4.3	1.9...6.7	4.2
C3, H5	2.3	2.2	2.6	2.7	0...4.3	2.4
N1, H7	−3.8	−3.8	−3.7	−3.4	−1.9...-3.7	−3.1
N4, H2	0.3	0.2	0.2	0.3		<1[a]
N4, H8	−2.6	−2.6	−3.2	−3.0	−1.9...-3.7	−3.1
C2, C5	2.1	2.1	1.6	2.2		2.0
C3, C6	3.2	3.2	3.5	3.5		∼0
C3, C8	0.4	0.4	0.1	0.2		1.0
C7, N4	−0.2	−0.2	−0.4	−0.3		<0.5[a]
N1, N4	0.0	0.0	0.0	0.1		∼0
Δ	1.8	1.7	1.9	1.6		0.0

[a] Experimental sign was not determined. The RMS error (Δ) was calculated only with measurable experimental constants ($|J| > 1$). [b] Usual values reported for peptides.[83]

constants at the N and C terminus of the dipeptide are reproduced by theory. For example, the constant $^1J(^\alpha C-^\alpha H)$ is higher at the N-end than at the C-end, ^1J(C2, H2) − ^1J(C5, H5) = 3.8 Hz, which is reproduced by the calculation, although the calculated difference (9.4 Hz at the B3L/IGLOII/PCM level) is rather overestimated. The observed differences ^1J(C7, H7) − ^1J(C8, H8) = 1.5, ^1J(C2, N1) − ^1J(C5, N4) = 2.0, ^1J(C2, C7) − ^1J(C5, C8) = −0.9 and ^1J(C2, C3) − ^1J(C5, C6) = −2.3 Hz are reproduced by the calculation as 2.7, 9.4, −1.7, and −0.6 Hz, respectively. Similar qualitative agreement can be seen for

Table 5. Experimental and Calculated Changes of Spin−Spin Coupling Constants (Hz) of LALA Caused by the Solvent Change ($\Delta = J(H_2O) - J(MeOH)$, in Hz) for Conformer **A**

J:	C7 H7	C8 H8	C3 H7	C6 H8	H2 H7	H5 H8	C7 H2	C8 H7	C2 H2	C5 H5
Δ_{expt}	0.8	0.8	0	0	0	0.2	−0.4	−0.3	1.5	0.8
Δ_{calcd}	0.65	0.83	0.09	0.01	−0.04	0.05	−0.36	−0.43	3.64	2.43

Table 6. Chemical Shifts and Spin−Spin Coupling Constants Most Affected by the Vibrational (Anharmonic) Averaging

		state averages			
	equilibrium value	|0>	|1>	|2>	experiment
		Shifts (ppm)			
C7	19.57	19.48	19.38	19.33	19.29
		Couplings (Hz)			
C3 H4	6.62	6.74	7.14	6.89	3.6
C2 H2	151.92	151.73	151.58	151.50	146.5
C3 C8	0.38	0.46	0.57	0.51	1.0

the two- (e.g., the experimental difference ^2J(C7, H2) − ^2J(C8, H5) = 0.4 Hz was reproduced as 0.6 Hz) and three-bond (^3J(H2, H7) − ^3J(H5, H8) is experimentally −0.2, theoretically 0.0 Hz) constants.

To validate the accuracy of the PCM solvent model, the LALA coupling constants were also calculated for methanol used as a solvent. For the measurement, the methanol solution used in the experiment contained 5% of water in order to stabilize the zwitterionic form in the solution. The calculated changes induced by the solvent effect are collected and compared with experiment in Table 5. As can be seen from the table, the theory accounts faithfully for the change in the solvent polarity. A somewhat larger deviation was obtained for the constants involving the α-hydrogen and carbon atoms (*J*(C2,H2), *J*(C5,H5)); this, however, can be expected as these groups are in a vicinity of the polar groups which may be involved in formation of the hydrogen bonds[29,84−86] or other specific solvent−solute interactions.

In Table 6 the effect of the vibrational averaging over the shifts and couplings (according to eq 2) is illustrated for a few selected NMR parameters (again in H_2O). Despite the large dispersion of the coordinates (cf. Figure 4) this effect is surprisingly small. As can be estimated from the values in Table 6, while the averaging can somewhat improve calculated values, this merit is minor in comparison with the overall inaccuracy of the calculations.

Chemical Shift Surfaces. To investigate their sensitivity to the geometry, the chemical shifts were calculated for the entire range of the φ, ψ angles (Ramachadran map). Although, as shown above, the presence of multiple conformers in the current LALA sample is not probable, these can be stabilized for longer peptides. In Table 7, the RMS differences (Δ) between the calculated and experimental values are summarized for the four energy minima (**A**, **B**, **C**, **D**, cf. Figure 3, Table 1). Additionally, average deviations (δ) over the 36 conformers homogeneously covering the Ramachadran surface are given in the sixth column of Table 7. We see, for example, that the amide hydrogen and nitrogen (H4, N4) atoms are quite sensitive to the geometry changes and can be potentially used as probes of peptide

Table 7. Errors of Calculated (B3LYP/IGLOII/PCM) Chemical Shifts for the LALA Conformers[a,b]

	$\sigma_{cald} - \sigma_{expt}$ (ppm)				
nucleus	**A**	**B**	**C**	**D**	δ
H1	−0.8	−0.7	−0.9	−0.9	0.1
H2	0.3	0.2	0.3	0.2	0.1
H4	−0.6	−1.1	−1.1	−1.4	0.6
H5	−0.1	−0.5	−0.1	−0.5	0.2
H7	−0.1	0.0	0.1	0.1	0.1
H8	−0.1	0.1	−0.1	0.0	0.2
C2	9.3	8.9	14.3	14.4	1.7
C3	3.3	4.4	1.8	2.7	1.0
C5	5.5	8.4	5.1	8.4	2.1
C6	3.5	2.8	3.9	2.9	0.7
C7	2.4	3.0	1.4	1.0	1.6
C8	3.6	−0.5	3.5	−0.6	1.1
N1	−34.7	−35.3	−35.0	−34.1	1.3
N4	−21.9	−27.8	−27.6	−33.7	4.1
O3	59.9	70.4	107.1	119.0	17.7
O6	60.9	64.9	62.3	65.6	8.7
Δ	3.7	4.0	4.7	5.0	

[a] Δ: RMS error without oxygen and nitrogen atoms. [b] δ: average absolute deviation from the mean value over the entire PES surface, $1/N \sum_{i=1..N}|\Delta\sigma_i - \bar{\sigma}|$, where $N = 36$ conformers, $\Delta\sigma_i = \sigma_{calcd,i} - \sigma_{expt}$ is the deviation for the *i*-th grid point from experiment (no temperature/Boltzmann averaging used).

conformations. On the other hand, somewhat surprisingly, chemical shifts of the αC-hydrogens (H2, H5) appear almost unaffected by the geometry variations. Interestingly, chemical shifts of the α-protons and α-carbons were suggested as probes for NMR detection of the β-sheet and helical fragments in proteins by Wishart as the Chemical shift index (CSI) method.[87] For the LALA shifts, however, only of the α-carbons (C2, C5) exhibit convincing φ,ψ variations, which can be perhaps explained by the absence of the α-hydrogen H-bond acceptor, present in β-sheets.[88,89] The hydrogens and carbons of the C-terminus (H5, C5) of the peptide seem to be more sensitive to the conformation motion than those at the N-terminus (H2, C2). A modest dependence of the chemical shifts on the angle variation is exhibited also by the methyl hydrogen atoms (H7, H8), while the methyl carbon (C7, C8) shifts vary more. In fact, all the heavy atom shifts except the terminal nitrogen (N1) significantly change with the φ,ψ angles.

Apart from the average deviations and variances, we can distinguish different conformational behaviors of the shifts according to their different dependences on the two angles φ,ψ. This is illustrated by Figure 7, where the calculated surfaces for the C2, C5, H4, and N4 atom shifts are plotted. Clearly, the shift of C2 depends on the ψ, and the shift of C5 depends on the angle φ only. Such "one-dimensional" simple dependences can perhaps be better used for conformational monitoring than those of H4, N4 given in the lower part of Figure 7. The N−H group lies between the φ,ψ rotating bonds and is understandably

(84) Pecul, M.; Sadlej, J. *Chem. Phys.* **1998**, *234*−*119*, 111.
(85) Bouř, P.; Michalík, D.; Kapitán, J. *J. Chem. Phys.* **2005**, *122*, 144501 1−9.
(86) Bouř, P. *J. Chem. Phys.* **2004**, *121* (16), 7545−7548.
(87) Wishart, D. S.; Sykes, B. D. *J. Biomol. NMR* **1994**, *4*, 171−180.
(88) Wagner, G.; Pardi, A.; Wuthrich, K. *J. Am. Chem. Soc.* **1983**, *105* (18), 5948−5949.
(89) Grzesiek, S.; Cordier, F.; Jaravine, V.; Darfield, M. *Prog. NMR Spectrosc.* **2004**, *45* (3−4), 275−300.

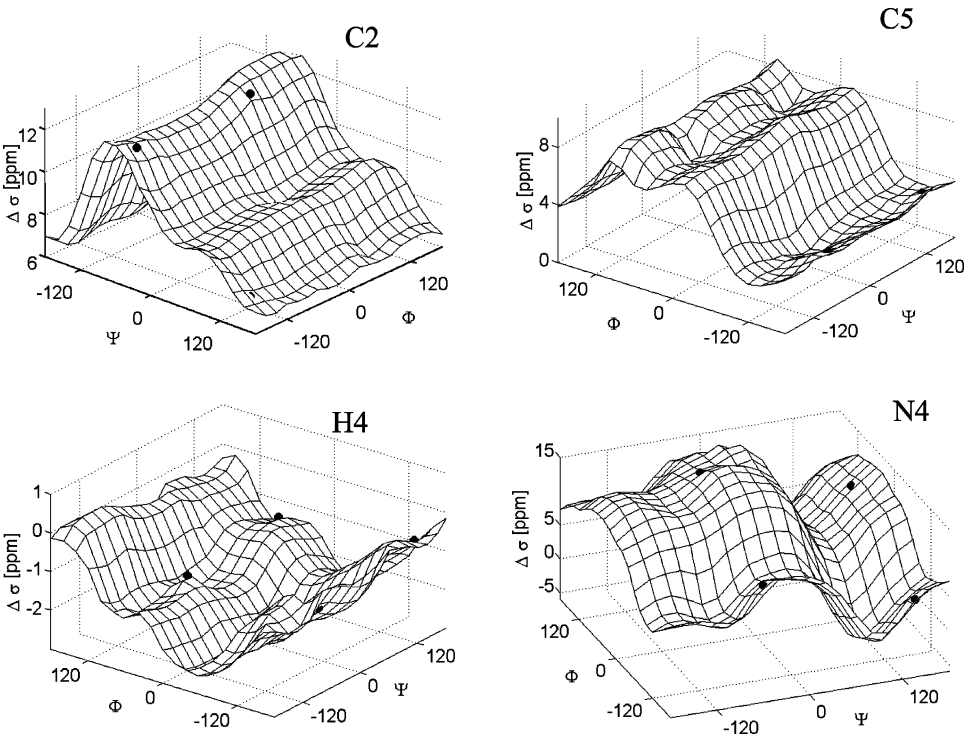

Figure 7. Examples of the dependence of the chemical shifts (plotted as deviations from experiment, calculated at the B3LYP/IGLOII/PCM level) on the torsion angles.

sensitive to both angles, providing more complicated surfaces. Thus we can "cross-validate" determination of the most abundant conformer in the sample, based on not only the errors found for individual conformers (in Table 7) but also on confronting the $\sigma(\varphi,\psi)$ shift surfaces with the pertinent experimental values. Similarly as C2, C5 and also the carbons C7 and C8 provide dependencies (not shown) allowing us to estimate the φ, ψ angles separately, while the variation of the carbonyl C3 and carboxyl C6 chemical shifts on the grid is small, which indicates their restricted applicability for resolution of the molecular structure. Additionally, the polarization of the C═O bond due to the solvent may influence the carbon chemical shift. Trial calculations with the ethanol and methanol solvents, however, revealed that such changes are minor in comparison to the geometry variations. However, the influence of the explicit hydrogen bonds not properly modeled here certainly contributes to the overall uncertainty regarding the conformer distribution (cf. Table 1) and NMR parameter precision (Tables 3, 4). This is somewhat regrettable, since the ^{13}C═O shift was proposed as a probe of hydrogen bonding.[90] Clearly, better solvent models will be needed in the future.

Spin−Spin Coupling Surfaces. Similarly as for the shifts, the RMS errors of the calculated spin−spin coupling constants for the four conformers and their variance over the entire φ, ψ range were estimated and summarized in Table 8. Here we do not include small constants that could not be clearly determined experimentally. Apparently, as for the shifts, coupling constants calculated for the conformer **A** are closest to the experiment (Δ = 1.8 Hz). Occasionally, however, couplings calculated for the higher-energy conformers **B**−**D** may agree better with experiment than those of conformer **A**. This occurs namely for the constants involving atoms in the vicinity of the terminal charged groups. Although not regularly used as experimental probes of the peptide structure, even the direct constants involving atoms separated by one bond only (J(C2, H2), J(C5, H5), J(N4, H4), J(N1, C2), cf. δ in Table 8) are quite sensitive to the molecular shape. In terms of the relative values, however, the two-bond (geminal) and three-bond (vicinal) constants vary more. For example, for the deviation as defined in Table 7, δJ(C3, H5) = 2.4 Hz, which is about 100% of the observed value, while the biggest variation for the one-bond constants δJ(C5, H5) = 3.6 Hz, which is 2.5%. These variations of the couplings are in agreement with known ranges of these constants observed in peptides (see Table 4).[83]

Various types of the dependence of the coupling constants on the angles φ,ψ are documented by Figure 8, where the ^3J(C3, H5), ^3J(H4, H5), and ^1J(N4, H4) surfaces are plotted. The constants ^3J(C3, H5) and ^3J(H4, H5) predominantly depend on the φ angle. The constant ^1J(N4, H4) (in the lower part of Figure 8) pertains to the atoms between the φ, ψ rotating bonds and thus is dependent more on both the angles, similarly as in the case of the σ(H4), σ(N4) chemical shifts (Figure 7). Rather one-dimensional patterns were also found for the vicinal couplings ^3J(C3,H7) (ψ-dependence), ^3J(C6, H8) (φ-dependence), ^3J(H2, H7) (ψ) and ^3J(H5, H8) (φ), i.e., those comprising atoms localized in the vicinity of the rotating bond. Similarly, the ^2J(C3, H2) and ^2J(C6, H5) two-bond coupling maps enabled unambiguously validate the geometry of the predominant conformer. Maximal deviations of the calculated couplings from experiment on the geometry grid of −12.5, 3.5, and 6.1 Hz were observed for the ^1J, ^2J, and ^3J couplings, respectively. For some constants, however, no clear indication of a real conformation could be deduced, because the variation of the calculated couplings on the geometry was smaller than the overall precision.

(90) Xu, X. P.; Case, D. A. *J. Biomol. NMR* **2001**, *21*, 321−333.

Table 8. Errors of the Calculated Nuclear Spin−Spin Coupling Constants (Hz, Becke3LYP/IGLOII/PCM) for the Four LALA Conformers[a]

coupled nuclei	$J_{calc} - J_{expt}$ A	B	C	D	δ
		^1J:			
C7, H7	−1.3	−1.4	−1.5	−1.5	0.5
C8, H8	−2.5	−3.0	−2.5	−3.2	0.5
C2, H2	5.4	5.3	7.2	6.7	2.9
C5, H5	−0.4	−11.8	0.1	−12.5	3.6
N4, H4	0.0	0.0	1.8	2.3	2.1
C2, C3	0.9	0.3	3.7	3.2	1.2
C5, C6	−0.8	−1.9	−0.3	−1.7	1.0
C2, C7	1.0	1.0	0.3	0.4	1.8
C5, C8	1.8	5.9	1.6	6.5	1.3
C2, N1	4.0	3.8	8.3	8.5	2.1
C3, N4	−2.5	−2.9	−0.6	−0.6	1.3
C5, N4	1.6	2.0	1.8	2.2	0.7
		^2J:			
C2, H7	1.2	1.2	1.3	1.2	0.2
C5, H8	0.8	0.4	0.9	0.4	0.2
C5, H4	1.3	0.8	0.8	0.2	0.5
C3, H4	2.9	1.6	4.3	2.8	0.9
C7, H2	1.5	1.5	0.7	0.6	0.5
C8, H5	1.3	0.0	1.2	0.2	0.9
C3, H2	0.9	1.0	−2.2	−2.2	1.3
C6, H5	−0.4	−1.5	−0.4	−1.4	0.5
C2, N4	−3.7	−3.8	−1.6	−1.5	1.0
		^3J:			
H4, H5	0.1	1.2	0.6	0.9	2.5
H2, H7	−0.5	−0.4	−0.2	−0.1	0.1
H5, H8	−0.6	−0.2	−0.6	−0.2	0.3
C6, H4	2.2	0.4	1.7	0.2	1.7
C8, H4	−1.9	0.2	−2.0	0.1	0.2
C3, H7	0.3	−0.3	0.0	−0.1	0.2
C6, H8	−0.3	−0.6	−0.3	−0.6	0.2
C3, H5	−0.1	6.1	−0.2	5.8	2.4
N1, H7	−0.7	−0.7	−1.0	−1.0	0.2
N4, H8	0.5	0.5	0.5	0.4	0.5
C2, C5	0.1	0.7	−0.8	−0.3	0.4
C3, C8	−0.6	−0.6	−0.6	−0.7	1.0
Δ	1.8	3.0	2.4	3.4	

[a] Constants that could not be reliably determined or were of unclear sign are not included. Symbols Δ, δ are analogous to those in Tables 3, 7.

Concluding Remarks. We believe that by studying the LALA dipeptide we have acquired useful knowledge that can be used for structural NMR studies of similar compounds. First, though the calculated molecular potential surface is rather inaccurate, it certainly leads to a wide dispersion of the torsion angles. Trial calculations indicate that less-polar solvents (methanol) may favor an even wider distribution of the angles φ,ψ. Thus the notion of "peptide conformation" has to be considered with caution. Interestingly, the latest studies indicate that such peptide and protein flexibility may be decisive for their biological role.[21,91,92] It is also interesting that the quantum and classical (MD) approaches give similar results in terms of the angle distribution; for LALA this seems to be a rather accidental result arising from a special form of the torsional potential and a strong interaction with environment. With the adiabatic approach limited to two coordinates, however, we do not have control over the possible influence of the rotation of the CH_3, NH_3, and CO_2 groups. These motions are too quick to be directly monitored by the NMR experiment.

Although the statistical analysis of the experimental and calculated NMR parameters are consistent with the conformer predictions based on the relative energies, the finite precision of the calculations of the chemical shifts and spin−spin coupling constants is clearly an issue that should be tackled in the future. Partly, the inaccuracy stems from the DFT approximation. It is known that only little improvement, if any, is achieved for the chemical shifts by existing DFT functionals, when comparing with the uncorrelated HF method. The reason is that reliable functionals involving electric current densities have not been developed yet. For the couplings, DFT performs much better than HF[93] but cannot be systematically improved in a similar way as the wave function-based configuration interaction methods. Obviously, application of the latter is prohibitive for larger systems. The other important source of the errors is an approximate accounting of the solvent effects. Some studies indicate that the continuum models may not be adequate for computation of the NMR parameters[29,84] and should be replaced by the cluster[94] or Car−Parrinello[95,96] models. However, in our case, when using a simple static inclusion of the explicit waters, we have obtained no convincing improvement. On the other hand, the application of the continuum model seems essential for the accuracy of the computations. Not only, as pointed out above, the zwitterion is not computationally stable in a vacuum, but if calculated with fixed geometry the vacuum shifts and coupling constants are significantly less accurate. These shift changes are relatively minor for the C and H atoms (see corresponding table in the Supporting Information) and still enable one to discriminate between individual conformers. For the couplings, vacuum values obtained in this way would be quite unreasonable (for a control computation, the RMS error $\Delta = 1.8$ Hz for the B3L/IGLOII/PCM method in Table 4 rose to 25.5 Hz!). Fortunately, the computations of the NMR parameters within the PCM are only moderately slower (by ∼20%) than if done in a vacuum.

The effect of the anharmonic averaging of the NMR parameters appears to be overshadowed by other inaccuracies. Perhaps anharmonic effects in higher-energy vibrational modes involving covalent-bond changes (ignored in this study) provide bigger corrections. However, note that small changes in the average values do not automatically indicate "harmonicity". In the future, other techniques such as optical spectroscopies, providing not only averaged values but also the dispersion of physically observable properties, may map the energy surface more directly. Despite these and other remaining conceptual problems, the analyses clearly enabled us to determine the molecular conformation and to estimate which chemical shifts and coupling constants are most useful for a peptide structural determination. Certainly, two-dimensional sections of the total property surfaces make the prediction more reliable than a standard analysis based on the equilibrium structure approach.

(91) Plaxco, K. W.; Gross, M. *Nature* **1997**, *386*, 657.
(92) Uversky, V. N. *Proteins* **2000**, *41*, 415−427.
(93) Bouř, P.; Buděšínský, M. *J. Chem. Phys.* **1999**, *110*, 2836−2843.
(94) Malkin, V. G.; Malkina, O. L.; Steinebrunner, G.; Huber, H. *Chem.—Eur. J.* **1996**, *2*, 452−457.
(95) Pfrommer, B. G.; Mauri, F.; Louie, S. G. *J. Am. Chem. Soc.* **2000**, *122*, 123−129.
(96) Pennanen, T. S.; Vaara, J.; Lantto, P.; Sillanpaa, A. J.; Laasonen, K.; Jokisaari, J. *J. Am. Chem. Soc.* **2004**, *124*, 11093−11102.

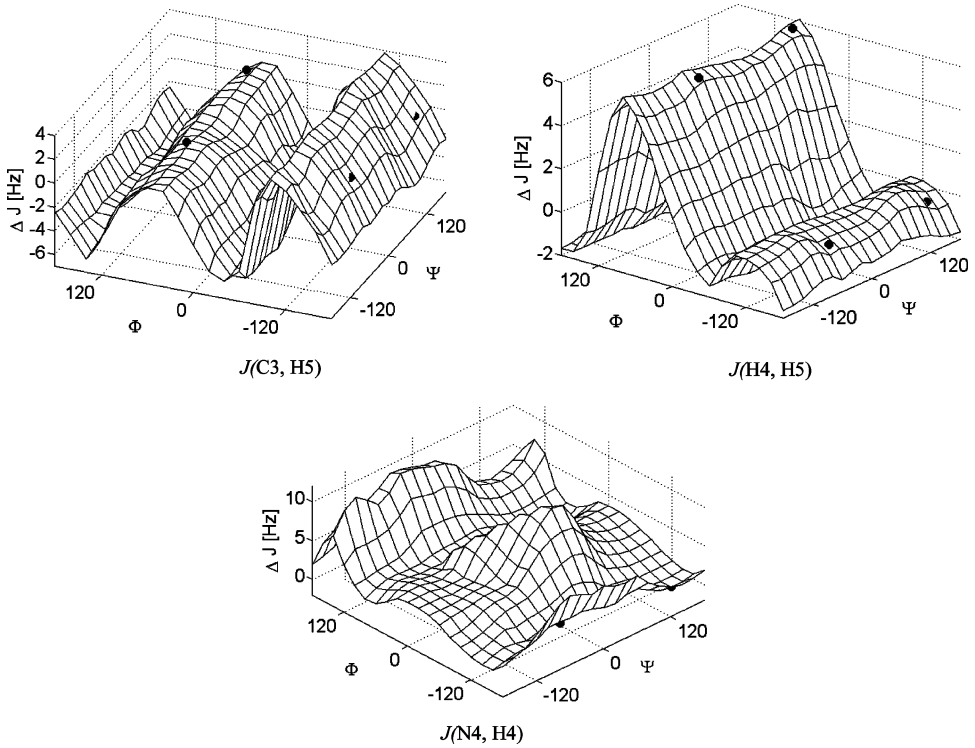

Figure 8. Examples of the dependence of the spin−spin coupling constants on the torsion angles. Deviations of calculated values (B3LYP/IGLOII/PCM) from experimental constants are plotted.

Summary

All chemical shifts and detectable direct, geminal, and vicinal coupling constants were measured for isotopically labeled isomers of LALA. With the aid of ab initio simulations of the NMR parameters and their dependence on the molecular geometry, grid variables most sensitive to the geometry were determined. The NMR data analysis is consistent with the theoretical molecular potential-energy surface and the classical and quantum modeling. Only one prevalent conformer of LALA is present in the sample, approximately corresponding to the X-ray crystal structure data. Although the main chain torsion angles may vary almost freely in a relatively wide range, this motion has little effect on the actual values of the chemical shifts and spin−spin couplings.

Acknowledgment. This work was supported by the Grant Agency of the Academy of Sciences (A4055104) and by the Grant Agency of the Czech Republic (203/05/0388).

Supporting Information Available: Complete ref 59, Cartesian coordinates (B3LYP/6-311++G**/PCM) of the conformer **A** of LALA, and errors of the shifts obtained by a control vacuum computation. This material is available free of charge via the Internet at http://pubs.acs.org.

JA0552343